Computer Simulation of a Fire-Ball

Yoshihiro SATO, Tomotake YANAGITA* and Naofumi OGITA**

Science and Engineering Research Laboratory
Waseda University, Tokyo
* *Faculty of Engineering Science, Osaka University*
Toyonaka, Osaka
** *The Institute of Physical and Chemical Research*
Wako, Saitama

(Received Januany 20, 1971)

A computer simulation is made on multiple pi-meson emission from a fire-ball under rigorous requirement of the energy-momentum conservation and basic assumptions on its physical properties, which were obtained from the superposed data of C-jets of the Chacaltaya emulsion chamber experiment. The computer constructed about one thousand examples each for cases of the fire-ball rest-mass, 2.2, 2.4, 2.6 and 2.8 GeV/c^2 with the width of 100 MeV/c^2.

Further, the simulation experiment is carried out on the C-jet observation by the producer emulsion chamber under the identical conditions with the real experiment of Chacaltaya Chamber Nos. 12 and 13. Through the simulation experiment, one is able to perform detailed investigation on the fluctuation problem and the experimental biases in measurement and analysis on the individual events.

Comparison of the data of artificial C-jets and of experimental C-jets provides a method of estimation of a fire-ball rest-mass. This comparison is made on distributions of the three physical quantities of the event, the γ-ray mass (total energy released into γ-rays in the fire-ball system), the invariant mass of the detected γ-rays and the γ-ray multiplicity. Those three quantities are affected in different ways by the experimental conditions, so that their mutual consistency check allows to discuss accuracy of the mass estimation and possible systematic errors in the experimental data. The conclusion from the comparison of 70 C-jet events of the Chacaltaya experiment with the artificial ones is that the fire-ball mass-value lies between 2.2 and 2.6 GeV/c^2. In addition, the present work gives suggestions on design of the experiments and method of the analysis.

§1. Introduction

During the period of 1965～67, the Japan-Brazil collaboration group made exposure of emulsion chambers with the jet producer layer—called Chamber No. 12 and No. 13—at the Chacaltaya cosmic-ray observatory, aiming at precise measurement on jets of extremely high energy. Results of the analysis of the experimental data[1] are showing us that phenomena of multiple production of mesons in the observed interval of their radiated energy, $\sum E_\gamma = 3 \sim 20$ TeV, are occurring through emission of fire-balls with nearly constant mass (2～3 GeV/c^2). In parallel to this cosmic-ray work, Hasegawa, Nanjo, Ogata, Sakata, Tanaka and Yajima[2] made investigation on the multiple meson produc-

tion phenomena in the energy region near the threshold of fire-ball production, in order to make clear the production mechanism of a fire-ball. They made an analysis on multi-prong events in photographs of the bubble chamber with π^--meson beam of 10 GeV/c and also on jet events in nuclear emulsion stacks exposed to proton beam of 22.6 GeV/c and of 24 GeV/c. They found that the multiple production in these low energy regions is also occurring through the production of a fire-ball, too, and they gave estimation of the fire-ball mass as 2.4 ± 0.4 GeV/c^2.

After having evidences on the production of a fire-ball over a wide region of energies, one direction of our study is to investigate the essence of the fire-ball in its relation to new phenomena seen in still higher energy regions. The other is, of course, to perform a more accurate and precise study on physical properties of the fire-ball for obtaining a clearer idea on this newly discovered substance —a fire-ball.

It has been generally believed in these twenty years that the cosmic-ray experiment rarely gives quantitative results to a problem on elementary particles, mainly because energies of the concerned cosmic-ray phenomena is becoming higher and higher and the primary cosmic-rays have a steep energy spectrum. Thus the experiment on extremely high energy phenomena is always with difficulties of poor statistics and complicated experimental biases. Though the emulsion chamber experiment overcame a part of the difficulties through concentrating the effort on a measurement of particles of the electromagnetic component and π^0-mesons, it is not an exception nor a "complete" experiment. There are repeated proposals among us to improve the experiment so as not to be confined to π^0-meson observation but to include simultaneous observation on charged π-mesons and other particles.

Now, the Chacaltaya experiment is successful in obtaining nearly one hundred events of a nuclear interaction in the producer layer (called the C-jets). We have quantitative results on various physical quantities through the analysis on the statistically superposed data of the C-jets, and the results are found to be consistent with the H-quantum hypothesis[8]—emission and decay of a fire-ball of constant mass, $2\sim3$ GeV/c^2. But it is on the average character of the phenomena. It is required to perform detailed analysis on each of the individual events before arriving at a conclusion on the fire-ball problem. A preliminary study along this direction was made in the accompanying paper of the collaboration, but it remained rather in a qualitative stage because no quantitative estimation was given to the error.

Since the Chacaltaya experiment has arrived at such a level of the investigation, we think that a further critical study on the experimental data will give a clue towards the "precise" cosmic-ray experiment. It is first to learn essence of the fluctuation phenomena of multi-meson emission from a fire-ball, and then to apply the knowledges to analysis of the experimental

data. Here, one should keep in mind the existence of the experimental biases caused by the method of detection and the cosmic-ray energy spectrum.

The above are motivation of our simulation experiment with a computer on C-jets observed by a producer chamber. We impose some basic and simple assumptions on properties of a fire-ball, all of which were already experimentally confirmed in a statistical way. Mass of a fire-ball, M_0, is left as a parameter, and the simulation is carried out in the four cases of different mass-values, $M_0=2.2$, 2.4, 2.6 and 2.8 GeV/c^2. With data of the simulated examples of emission of π-mesons from a fire-ball thus constructed, we make a simulation experiment on the artificial C-jets under the indentical conditions with the Chacaltaya experiment. Comparison of results from the artificial C-jet data with those from the experiment offers precise knowledges on physical properties of a fire-ball. In addition, the simulation study gives suggestions for a future method of analysis through a detailed examination on various experimental biases.

In §2, we describe the basic assumptions, the procedure of computation, and a check on the statistical results of the present simulation experiment. Section 3 is for discussions on various origins of fluctuation of the phenomena and the possibility of mass-estimation of a fire-ball. Then a conclusion is derived on the estimated mass-value of a fire-ball through comparison of the experimental data and the simulated data. In addition, a discussion will be given on the effect of biases and possible contaminations in the experiment.

Section 4 concerns with further problems on the C-jet analysis, and a proposal is made on method of examination on the individual C-jet data. In §5, we describe a conclusion of the present simulation study and suggestions for the future experiment.

§2. Method of the simulation

Artificial C-jets are constructed by the following procedure for comparison with the observed C-jets by Chambers 12 and 13 of the Chacaltaya emulsion chamber experiment. First, we make about one thousand simulated examples of isotropic emission of a number of π-mesons from a fire-ball with a certain mass value. Then, with use of a set of data of the simulated fire-balls, we construct examples of the artificial C-jet under an assumption of energy spectrum of the incoming cosmic-rays and simulated conditions of the experiment.

Construction of simulated fire-ball data We make the following three basic assumptions on properties of a fire-ball.

Assump.-1. Mass of a fire-ball M_0 is assumed as a constant.

The calculations are made for four cases with $M_0=2.2$, 2.4, 2.6 and 2.8 GeV/c^2.

Assump.-2. A fire-ball decays into a number of π-mesons. In the fire-ball

rest system, the emission of π-mesons is isotropic with the momentum distribution as*)

$$f(p^*)dp^* = (p^*/p_0^2)\exp(-p^*/p_0)dp^* \quad \text{with} \quad p_0 = 175\text{MeV}/c. \tag{1}$$

Assump.-3. An emitted π-meson has probability 1/3 to be neutral.

The calculations are made only with the conservation law of energies and momenta besides the above assumptions. As will be found from the following procedure of the computation, the data of artificial "fire-balls" are constructed from the simulated examples satisfying the conservation law of energies and momenta with good accuracy.

Step-1. Magnitude of momentum of an emitted π-meson, p_i^*, is sampled randomly from the distribution given by Eq. (1). The total energy sum of successively emitted π-mesons, $\sum_{j=1}^{N} E_i^*$, is constructed. As soon as the sum $\sum_{i=1}^{N} E_i^*$ of N π-mesons fall into the interval defined as $M_0 \pm \pi$-meson rest mass (135 MeV/c^2), the sampling procedure is completed and the computation advances into the next step. On the other hand, if the sum $\sum E_i^*$ happens not to fall into the allowed interval but to jump it over, the computed results are discarded and the simulation procedure is started again from the beginning.

Step-2. A set of emission angles, $\cos\theta_i^*$ and ϕ_i^* $(i=1, 2, \cdots N)$, of the emitted N π-mesons in the fire-ball rest system are sampled from uniformly distributed random numbers. The total vector sum of the momenta, $\sum_i \boldsymbol{p}_i^*$, is constructed, and we impose the following criterion on the vector sum,

$$|\sum_i \boldsymbol{p}_i^*| < \pi\text{-meson rest mass (135 MeV}/c^2). \tag{2}$$

Sampling of the emission angles, $\cos\theta_i^*$ and ϕ_i^* $(i=1, 2, \cdots N)$ is repeated until the above criterion is satisfied. If the above criterion is found not to be satisfied after the repetitions of sixty times, the computed results are discarded and the simulation procedure is started again from Step-1.

With this procedure, we constructed 3,000 simulated examples of π-meson emission from a fire-ball each with the assigned mass value, M_0.

Step-3. In order to satisfy rigorously the conservation law of momenta, we make correction for momentum values of all the emitted π-mesons, substituting $\boldsymbol{p}_i^*$ by the following corrected values,

$$\boldsymbol{p}_i^* - \sum_{j=1}^{N} \boldsymbol{p}_j^*/N \to \boldsymbol{p}_i^*, \quad (i=1, 2, \cdots N) \tag{3}$$

*) The asterisk * represents quantities defined in the fire-ball rest system.

where N is the number of emitted mesons in an event.

Step-4. Mass of a fire-ball M is now calculated from the π-meson energies obtained by the corrected momentum value of Step-3, as

$$M=\sum_{i=1}^{N} E_i^*. \tag{4}$$

Out of 3,000 examples constructed by Steps 1~3, we select only those which satisfy the criterion,

$$|M_0-M|\leq 0.05 \text{ GeV}/c^2, \tag{5}$$

and make a set of simulated fire-ball data for further use.

The second column of Table I shows the number of examples in the thus constructed set of simulated fire-ball data each for the assigned mass-value M_0. Distributions of mass-values of the simulated fire-balls of each M_0-group are of rectangular shape with its center at M_0 and width of 0.1 GeV/c^2.

Step-5. We make assignment of a charge state for all of the emitted N π-mesons with use of a uniform random number, giving a probability of 1/3 to be neutral. Since the required statistics for further use is very large, the procedure of charge assignment is applied three times for each example in the set of simulated fire-ball data and it permits to increase the statistics three times.

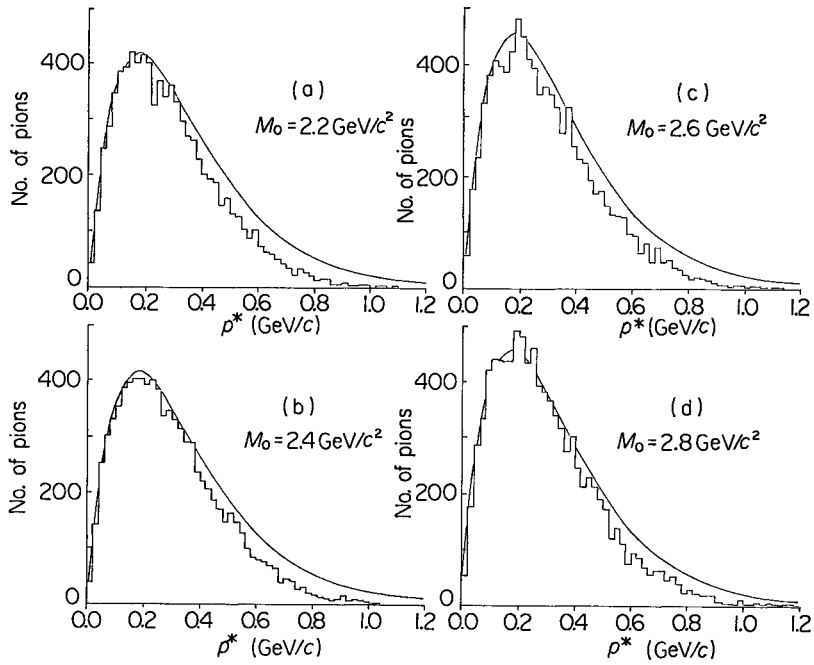

Fig. 1. Pi-meson momentum distributions in the fire-ball rest system. Figures (a), (b), (c) and (d) correspond to mass values M_0=2.2, 2.4, 2.6 and 2.8 GeV/c^2. Solid curves show the assumed distribution.

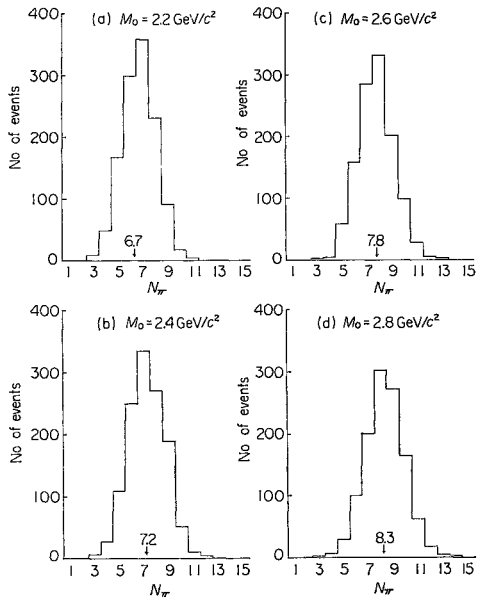

Fig. 2. Number distributions of π-mesons decaying from a fire-ball.

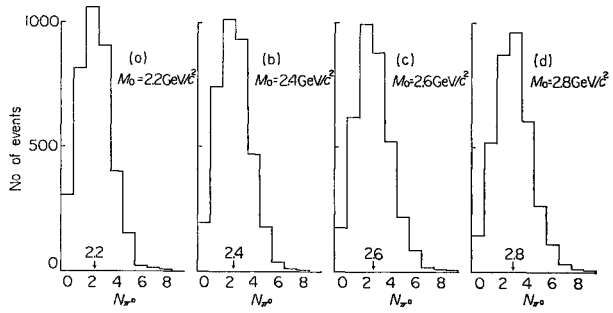

Fig. 3. Number distributions of π^0-mesons decaying from a fire-ball.

A check of the above simulation procedure was made by constructing a distribution of p^*, N_π, and N_{π^0} for each M_0-group of the simulated fire-ball data. The results are shown in Figs. 1~3. As is seen in Fig. 1, the distribution of p^* has a slight deviation in the high momentum region from the originally assumed distribution (1). It is due to a restriction from the conservation law of energies and momenta.

Simulation of C-jets Construction of artificial C-jets is carried out with a hypothetical chamber shown in Fig. 4, which has essentially the same structure as Chambers 12 and 13 of the Chacaltaya experiment. We impose the following two additional assumptions for the simulation procedure.

Assump.–4. Production frequency of a fire-ball is a function of depth x in the producer layer, such as

$$f(x)dx \propto \exp(-x/L)dx, \tag{6}$$

where L is a mean free path of a nuclear collision. The direction of motion of a fire-ball is always assumed as vertical to the emulsion chamber plane.

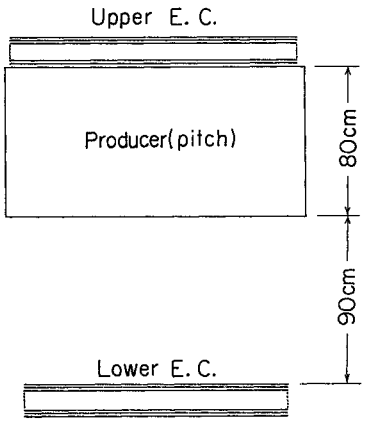

Fig. 4. Illustration of design of an emulsion chamber assumed in our simulation experiment.

Assump.–5. Distribution function of a Lorentz factor γ_f of a fire-ball in the laboratory system is given in the integral form as γ_f^{-2}. Our intention is to have the artificial C-jet data to be compared with the experimental C-jet data of the Chacaltaya emulsion chamber, without going into complicated and sometimes ambiguous arguments on the primary cosmic-ray spectrum and the inelasticity. Therefore we are satisfied, for the moment, with reproducing the experimentally known integral spectrum of the amount of the radiated energy of nuclear interaction as

$$f(\sum E_\gamma) \propto (\sum E_\gamma)^{-2}. \tag{7}$$

With those assumptions, the simulation procedure can be formulated as follows:

Step–6. For the location of production of a fire-ball, we sample its depth x in the producer layer by the formula

$$x = -L \ln u, \tag{8}$$

where u is a uniform random number.

Step–7. A value of Lorentz factor of a fire-ball is sampled as

$$\gamma_f = \gamma_{f\min}/u^{1/2}, \tag{9}$$

where $\gamma_{f\min}$ is the minimum value of the Lorentz factor. Its numerical value is put as small as $\gamma_{f\min}=800$ in order to avoid the effect of the minimum value $\gamma_{f\min}$ in comparison of the simulated C-jet data with the experimental one, where the selection criterion of the events is imposed as $\sum E_\gamma \geq 3$ TeV.

Step–8. Decay process of a π^0-meson into two γ-rays is simulated and all quantities of the γ-rays are transformed into the laboratory system, com-

Table I.

Assumed mass of a fire-ball M_0 (GeV/c^2)	Number of artificial fire-balls	Number of artificial C-jets	Number of C-jets under conditions: $\Sigma E_\gamma \geq 3$ TeV, $n_\gamma \geq 4$ ($E_{min}=0.2$ TeV)
2.2	1222	3666	163
2.4	1189	3567	160
2.6	1170	3510	190
2.8	1171	3513	233
Chacaltaya experiment	Normal	62	75
	Two fire-ball type	7	
	Anormalous (T)	5	
	Anormalous (SH)	1	

Anormalous events with (T) are those called torpedo and one with (SH) is with $\Sigma p_{T\gamma} > 2.5$ GeV/c.

puting their energy and location at the lower chamber.

Table I gives the total number of the artificial C-jets constructed by the above procedure, and also their number under the following selection criteria; take only γ-rays with energy greater than the detection threshold $E_{min}=0.2$ TeV and pick up only those C-jets with $\Sigma E_\gamma \geq 3$ TeV and $n_\gamma \geq 4$. These selection criteria are identical with those applied in the experimental analysis of the Chacaltaya emulsion chamber experiment, and they are applied to the artificial C-jets, too, for the comparison. Hereafter, we will consider only those C-jets selected under the criteria, unless it is specifically stated.

Check of the statistical results of the simulated C-jets

Figure 5 presents ΣE_γ spec-

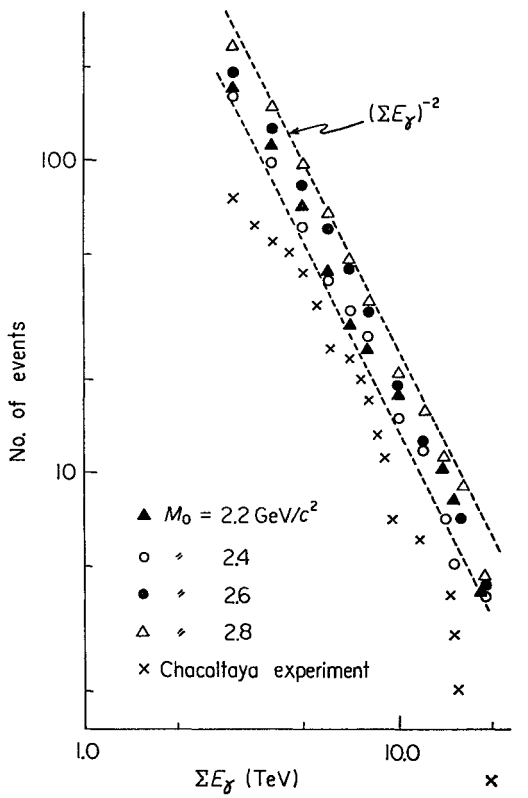

Fig. 5. Integral distributions of the total radiated energies, ΣE_γ, of C-jets in the Chacaltaya experiment and our simulation experiment. Broken lines show the power spectrum of a form, $(\Sigma E_\gamma)^{-2}$.

trum of the artificial C-jets of the four M_0-groups. The simulated results in all the cases are well fitted by a power spectrum of $(\sum E_\gamma)^{-2}$ in the concerned energy region, $\sum E_\gamma \geq 3$ TeV, because of the assumed power spectrum $(\gamma_f)^{-2}$ of the Lorentz factor. The experimental results on the $\sum E_\gamma$ spectrum are also plotted together in the same figure. The experimental ones show deviation from the power spectrum, $(\sum E_\gamma)^{-2}$, particularly near the lower limit of the selection, $(\sum E_\gamma)_{\min}=3$ TeV. This will be partly from statistical fluctuation due to its small observed number and also from some scanning inefficiency and experimental biases.

In the Chacaltaya experiment, analysis was made dividing the observed C-jets into four groups of different $\sum E_\gamma$ intervals. The artificial C-jets are also divided into groups of the same $\sum E_\gamma$ intervals for the comparison. Figure 6 presents integral distribution of normalized energy of γ-rays, $E_\gamma/\sum E_\gamma$, for the four groups of the artificial C-jets. The distribution in an integral form can be well fitted by an exponential function as

$$F(E_\gamma, \sum E_\gamma) = N_\gamma \exp(-N_\gamma E_\gamma / \sum E_\gamma), \tag{10}$$

in all of the groups of different $\sum E_\gamma$ intervals and of different M_0-values. They are in agreement with the experimental distribution, too, except in a region of very small $E_\gamma/\sum E_\gamma$, where one should expect effects of various

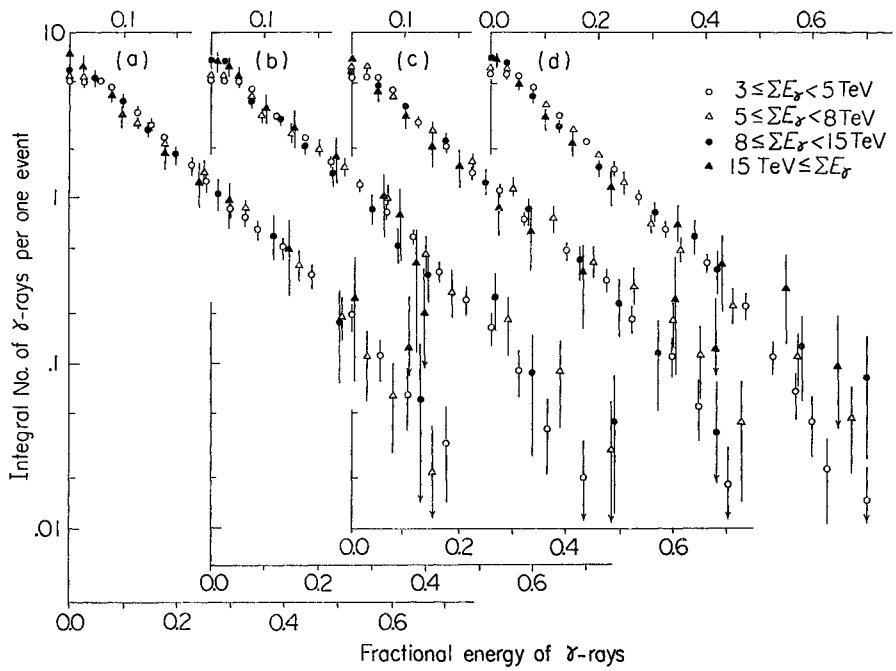

Fig. 6. Integral distributions of the fractional energies of γ-rays, $E_\gamma/\sum E_\gamma$, obtained in our simulation experiment.

experimental biases. An extrapolation of the $E_\gamma/\sum E_\gamma$ distribution towards zero energy gives a value of N_γ in (10), which is interpreted as a kind of average multiplicity of γ-rays emitted from a fire-ball. It is remarkable that a value of N_γ is always found in an interval 7.5 ± 0.5 even if the assigned mass of a fire-ball M_0 varies from 2.2 GeV/c^2 to 2.8 GeV/c^2. Therefore it is concluded that a value of N_γ, which can be determined experimentally from the statistical analysis, is a quantity rather insensitive to a mass-value of a fire-ball.

The center of an artificial C-jet is defined as the energy-weighted center of locations of γ-rays, in the same way as in the experimetal analysis, and transverse momentum of the γ-rays is computed referring to this center. Distribution of the transverse momentum is found not varying with an assumed value of M_0, so we present the distribution in Fig. 7 only for cases with $M_0=2.4$ GeV/c^2. A curve in the figure shows the theoretical distribution which is obtained analytically from the γ-ray mometum distribution as

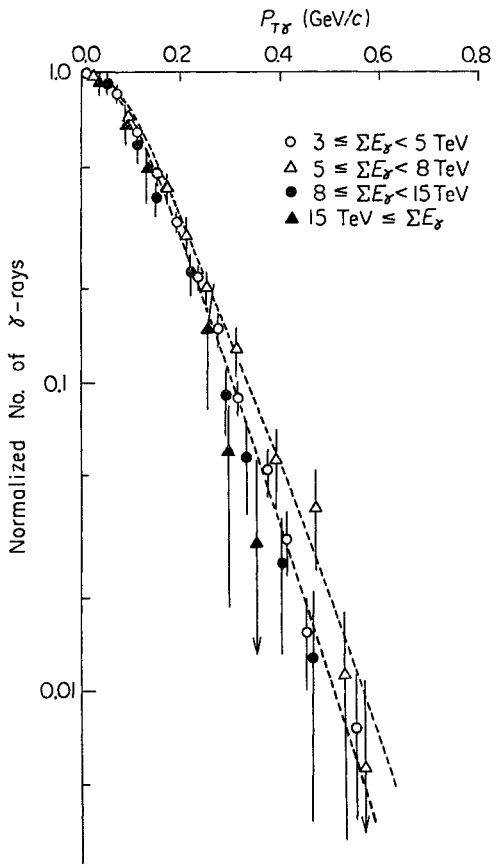

Fig. 7. Integral distribution of transverse momenta of γ-rays, $p_{T\gamma}$, obtained in our simulation experiment with $M_0=2.4$ GeV/c^2.

$$f(p_\gamma^*)dp_\gamma^*d\Omega=(p_\gamma^*/p_0^2)\exp(-p_\gamma^*/p_0)dp_\gamma^*d\Omega^*, \tag{11}$$

where values of p_0 are assumed as $p_0=80$, 90 MeV/c. One sees good agreement between them, as expected.

§3. Estimation of fire-ball mass

Through the statistical analysis of the Chacaltaya emulsion chamber experiment, we disclosed the existence and some physical properties of a fire-ball.

There, the analysis was made on the basis of measurement of quantities which are insensitive to the fire-ball mass value. Some of the results were already as basic assumptions of the present simulation procedure, where we left mass of a fire-ball as a variable parameter.

As a next step in the experiment, an analysis was made on the individual C-jets for obtaining estimation of the fire-ball mass. Comparison of results of this analysis on the individual events with the simulated ones will be important in various aspects. First, one will be able to see whether the average properties mentioned above are consistent with all of the observed individual events. Second, one will be able to make an accurate estimation of the fire-ball mass. Finally, one will be able to go into detailed arguments on effects of the experimental biases and examination on possible systematic errors, because the simulation experiment is providing information which cannot be obtained directly in the actual experiment.

Selection criteria for statistics of artificial C-jets In the analysis of the artificial C-jets, we impose the following selection criteria, which are also applied to the experimental C-jets, too.

i) Take only γ-rays with energy greater than $E_{\mathrm{min}}=0.2$ TeV; $E_\gamma \geq E_{\mathrm{min}}$.

ii) Multiplicity of γ-rays thus selected, n_γ, must be equal to or larger than four; $n_\gamma \geq 4$.

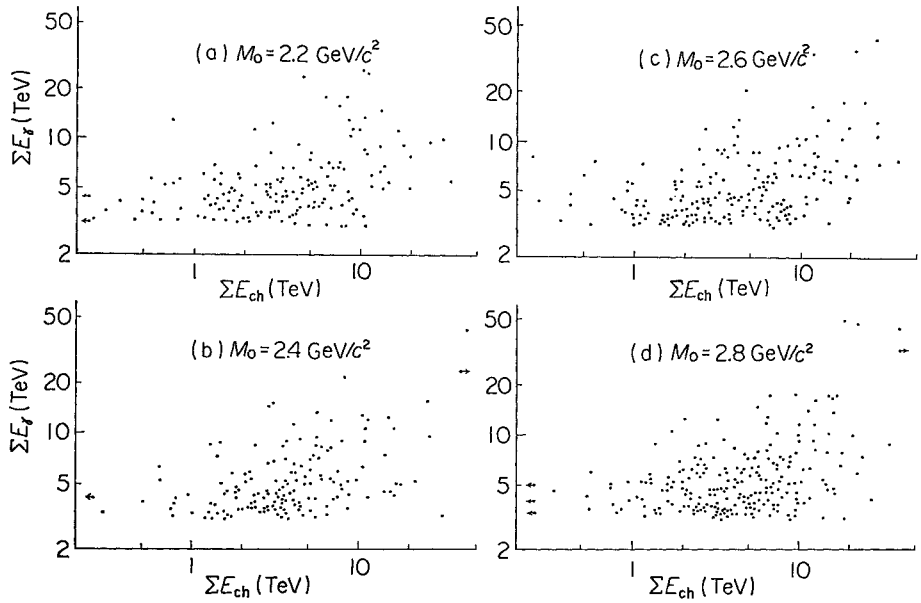

Fig. 8. Correlation diagrams between ΣE_γ and the total energies of charged π-mesons, ΣE_{ch}, in artificial C-jets.

iii) The energy sum of those γ-rays, $\sum E_\gamma$, must be equal to or larger than 3 TeV; $\sum E_\gamma \geq 3$ TeV.

Results of analysis on the selected C-jets will be significantly affected by the imposed criteria for selection, the steep energy spectrum of cosmic-rays and our method of observing only γ-rays out of the secondary particles from a fire-ball.

First, we construct a correlation diagram between energy sum of the charged π-mesons, $\sum E_{ch}$, and of the detected γ-rays ($E_\gamma \geq 0.2$ TeV), $\sum E_\gamma$, in each artificial C-jet, and also a distribution of the ratio $\sum E_{ch}/\sum E_\gamma$. The results are presented in Figs. 8 and 9. One notices that dispersion of the points in the $\sum E_{ch}-\sum E_\gamma$ diagram is very wide. The dispersion is caused mainly by charge fluctuation of the emitted π-mesons, which is large because the π-meson multipicity is not great in case of a fire-ball with mass 2.2~2.8 GeV/c^2. The average value, $\langle \sum E_{ch}/\sum E_\gamma \rangle$, increases slowly as M_0 increases, because magnitude of the bias, due to the imposed selection criteria, increases as M_0 decreases. Therefore, errors can be quite large if one makes estimation of the total energy of an interaction by simply multiplying a certain constant factor to the observed value of $\sum E_\gamma$. It is particularly so in case of a fire-ball of mass as small as a few GeV.

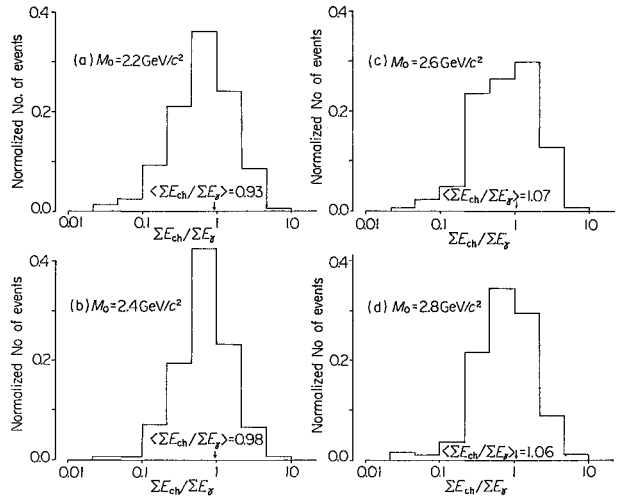

Fig. 9. Histograms of the ratio of $\sum E_{ch}$ to $\sum E_\gamma$ of artificial C-jets.

Distribution of $\mathfrak{M}_\gamma$, m_γ *and* n_γ In the analysis on individual C-jets of the Chacaltaya experiment, a new method for estimation of $\mathfrak{M}_\gamma$—amount of energy given to γ-rays from a fire-ball, hereafter called γ-ray mass of a fire-ball —was introduced and applied to all of the individual C-jets. The method was to make a comparison of the experimental data of a C-jet with the theoretical relation on $\sum_\theta E_\gamma - \theta_\gamma$ and $\sum_\theta p_{T\gamma} - \theta_\gamma$, which are derived from only an

assumption of isotropic emission of γ-rays from a fire-ball. The best-fit on $\sum_\theta E_\gamma - \theta_\gamma$ and $\sum_\theta p_{T\gamma} - \theta_\gamma$ relation gives an estimation of the γ-ray mass, $\mathfrak{M}_\gamma$, and the Lorentz factor γ of a fire-ball. Though the method has such shortcomings as the possibility of introducing subjective errors in the curve-fitting, or difficulty in making quantitative estimation of errors in the $\mathfrak{M}_\gamma$- and γ-estimation, it is a method which enables one to make a reasonable extrapolation of the data of a C-jet below the detection threshold, $E_{\min}$. Further, the two diagrams—one for $\sum_\theta E_\gamma$ and another for $\sum_\theta p_{T\gamma}$—which have different θ_γ-dependence are used, so that a cross-check between the two gives a reliability to the method. Now, for the simulated C-jets, a corresponding quantity to the γ-ray mass $\mathfrak{M}_\gamma$, is easily computed as energy sum of all the γ-rays in the fire-ball system, $\sum E_\gamma^*$.

Another important quantity used in the analysis on the individual C-jets is the invariant mass of detected γ-rays in a C-jet, m_γ, which is defined as

$$m_\gamma = [(\sum E_\gamma)^2 - (\sum p_\gamma)^2]^{1/2}. \tag{12}$$

In practice, we use a formula of the following form,

$$m_\gamma = [(\sum E_\gamma) \cdot (\sum E_\gamma \cdot \theta_\gamma^2)]^{1/2} \tag{13}$$

which is computed easily from the observed values of E_γ and θ_γ. Here, the emission angle θ_γ is measured from the energy-weighted center of detected γ-rays in a C-jet, and the same procedure is applied to the simulated C-jets, too. Contrary to a case of the γ-ray mass, $\mathfrak{M}_\gamma$, thus defined invariant mass, m_γ, is a quantity which can be computed unambiguously and is free from introduction of any subjective error, while it is bound to be affected directly by the detection threshold and the experimental biases.

The third quantity which can bring information on mass of a fire-ball is the multiplicity of γ-rays in a C-jet, n_γ. In the analysis of the Chacaltaya experiment, the quantity n_γ was not used because it would be directly affected by possible existence of scanning inefficiency and/or contamination of secondary effects. Further, the imposed selection criteria will give a governing effect on this quantity, n_γ. But, we will take this quantity into account in the present analysis for estimation of the fire-ball mass.

We construct the distribution of these three quantities $\mathfrak{M}_\gamma$ (or $\sum E_\gamma^*$), m_γ, and n_γ, for the artificial C-jets. In order to see the dependence of those quantities on varying mass-value of a fire-ball, we present in Fig. 10 comparison of the distribution in the two extreme cases of the assumed fire-ball mass-value, i.e., $M_0 = 2.2$ GeV/c^2 and 2.8 GeV/c^2.

As is seen from the figure, a tail of the distribution shows a characteristic variation with M_0 commonly for the three quantities. Whereas, variation of the distribution near the origin is different, since one sees a significant variation there only for the γ-ray mass distribution. The distribution of m_γ or n_γ

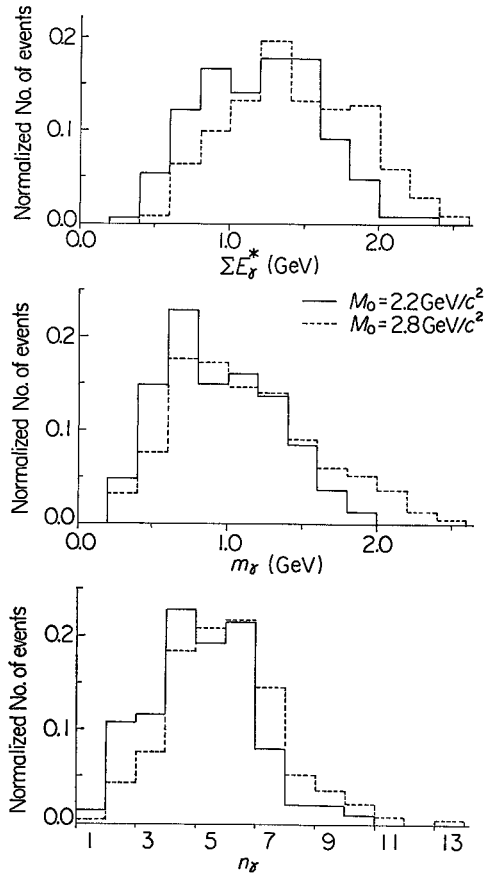

Fig. 10. Comparison of the histograms on artificial C-jets with M_0=2.2 and 2.8 GeV/c^2. (a): γ-ray mass of a fire-ball, ΣE_γ^*; (b) invariant mass of γ-rays, m_γ; (c) number of γ-rays, n_γ.

near the origin remains unchanged as M_0 varies, because the effect of the selection criteria governs the distribution in this region. We have already seen that the γ-ray mass, $\mathfrak{M}_\gamma$ (or ΣE_γ^*), is free from such a direct effect of the selection criteria. Therefore, one can conclude that a tail part of the distsibution in large mass (or multiplicity) region contains information on the mass-value of a fire-ball free from the experimental biases.

Variation of the multiplicity n_γ distribution with the fire-ball mass-value M_0 is not so apparent as for the other two quantities, $\mathfrak{M}_\gamma$ and m_γ. Table II shows average value of the multiplicity, $\langle n_\gamma \rangle$, for the artificial C-jets with various M_0, showing its slight variation.

Table II. Average multiplicity $\langle n_\gamma \rangle$.

Assumed mass of a fire-ball M_0 (GeV/c^2)	2.2	2.4	2.6	2.8
Average multiplicity of γ-rays ($E_\gamma \geq E_{\min}$)	5.4	5.4	5.6	5.9

Estimation of mass-value of a fire-ball Now, comparion is made on the distribution of $\mathfrak{M}_\gamma(\sum E_\gamma^*)$, m_γ and n_γ, between those from the simulation study and those from the experimental analysis, for obtaining estimation of mass-value of a fire-ball. The results are shown in Figs. 11, 12 and 13 for the three quantities, $\mathfrak{M}_\gamma$, m_γ and n_γ, where (a), (b), (c) and (d) in each of the figures express cases with the assumed mass-values, $M_0=2.2$, 2.4, 2.6 and 2.8 GeV/c^2, respectively. The histograms with solid lines represent the distributions obtained by the simulation study, while those with broken lines represent ones from the experimental analysis.

Above all, one finds, in all cases of the three concerned quantities, that the experimental distribution has a width around its maximum nearly equal to or narrower than that of the simulated distributions. It should be reminded that the simulated ones are obtained from the artificial C-jets constructed with data of examples of a fire-ball with a mass-value in a narrow interval, $M_0 \pm$

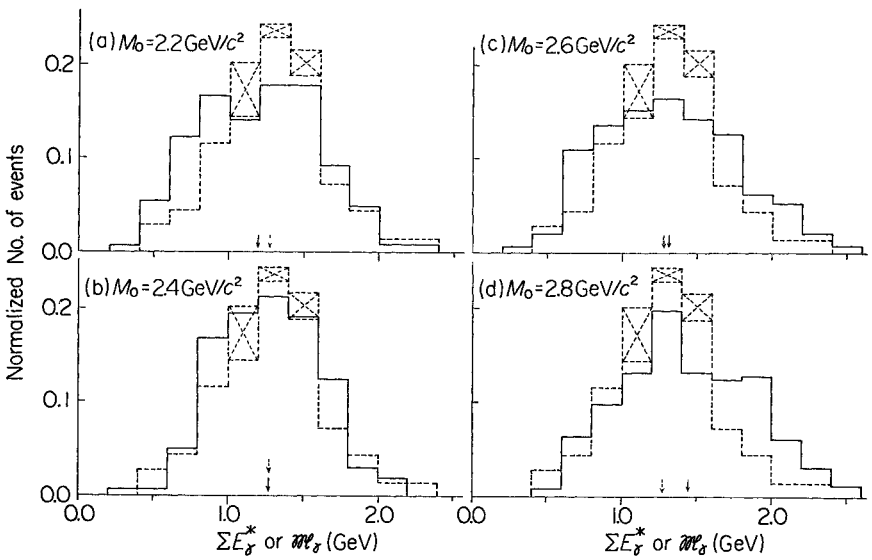

Fig. 11. Comparison of distributions of $\sum E_\gamma^*$ in our simulation experiment (solid line) and of $\mathfrak{M}_\gamma$ in the Chacaltaya experiment (broken line). The Chacaltaya events with crossed marks are of two-fire-ball type. Number of the Chacaltaya events cited here is 69 (normal 62+two-fire-ball type 7).

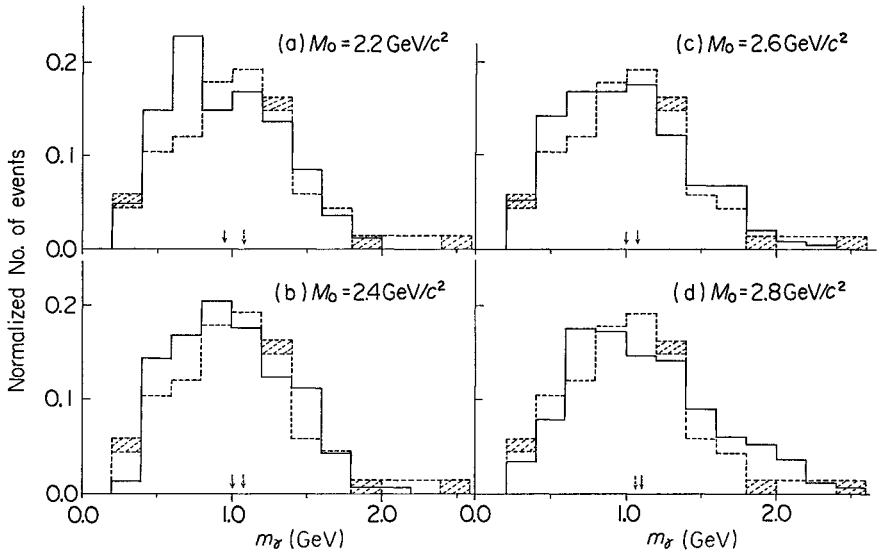

Fig. 12. Comparison of m_γ-distributions in our simulation experiment (solid line) and the Chacaltaya experiment (broken line). Chacaltaya events with shadow are anormalous events. Chacaltaya events cited here are 67 (normal 62+anormalous (T) 5). One anormalous (SH) event with large mass is omitted here. One of anormalous (T) event with m_γ=3.03 GeV is out of scale.

0.05 GeV/c^2. Thus the result is surprising, because one may expect that the experimental distribution would have a broader width than the simulated ones due to possible errors in the measurement.

Let us discuss in more detail on each of the distributions. The experimental $\mathfrak{M}_\gamma$-distribution is found in unexpectedly good agreement with the simulated $\sum E_\gamma^*$-distribution with M_0=2.4 GeV/c^2, as is seen in Fig. 11(b), while, for the m_γ-distribution, one is not able to find such a fine agreement of the experimental one with any of the simulated ones. But, reminding the above argument on significance of a tail part of the distribution, we can reject a possibility of M_0=2.8 GeV/c^2, because the case shows significant disagreement in the tail part with the experimental one. Now, the comparison on m_γ-distribution in the small mass region suspects existence of such systematic error in the experiment which causes under-estimation of frequency of the C-jets with small m_γ-value. We have already seen that the m_γ-distribution in this mass region is mainly determined by the imposed selection criteria, but not depending much on mass of a fire-ball. We will discuss later possible sources of systematic error together with other effects of the experimental biases.

From the above observation on the $\mathfrak{M}_\gamma$- and m_γ-distribution, we may conclude that mass of a fire-ball will lie in an interval between 2.2~2.6 GeV/c^2.

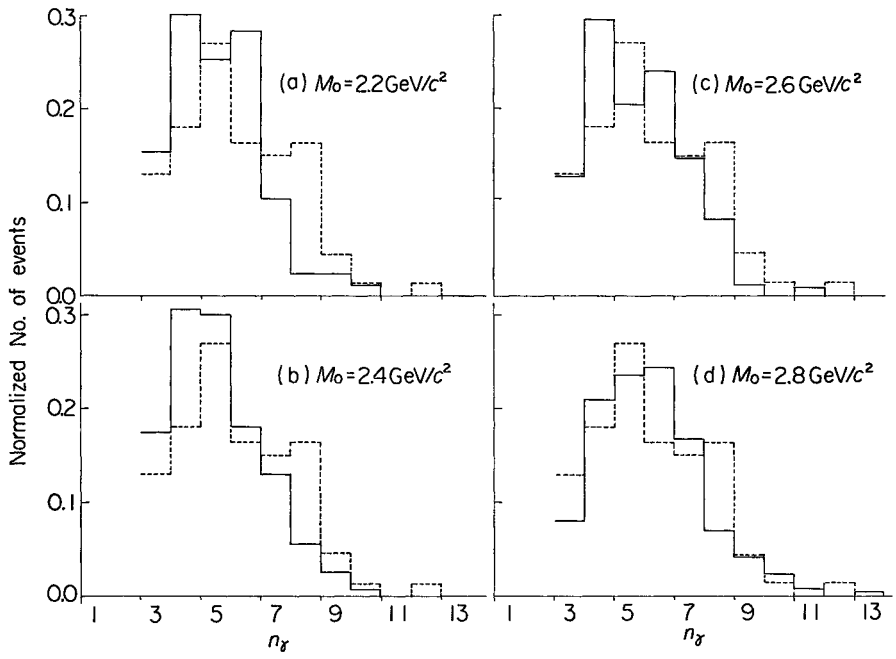

Fig. 13. Comparison of n_γ-distributions in our simulation experiment (solid line) and in the Chacaltaya experiment (broken line). Number of Chacaltaya events cited here is 67 (normal 62+anormalous (T) 5).

This conclusion can be checked further by examining the n_γ-distribution shown in Fig. 13. In the figure, we added, for a reference, frequency of the events with $n_\gamma=3$, which are discarded by the selection criteria. Agreement between the experimental and the simulated n_γ-distribution appears to be best in the case of $M_0=2.8$ GeV/c^2. But we already saw that the comparison on the $\mathfrak{M}_\gamma$- and m_γ-distribution is giving a different estimation of the M_0-value.

A slight difference is also seen between the average multiplicity of the experimental C-jets, $\langle n_\gamma\rangle=6.1$, and those of the simulated C-jets given in Table II. Both of the discrepancies are requiring careful examination on existence of possible systematic errors in the experimental data due to the scanning loss and the contaminations coming from various sources,—for example, mixing of "Pb-jets" among "γ-rays" in a C-jet, contribution of a successive nuclear interactions in the producer layer, effect of the succeeding fire-ball with smaller velocity, and so on. A final conclusion will be made only after examinining those points.

Scanning loss and its effect on the analysis The experimental $\sum E_\gamma$-spectrum of the C-jets of the Chacaltaya experiment, presented in Fig. 5 of §2, shows a significant deviation from a simple spectrum in low energy region near the minimum energy value, $\sum E_\gamma=3\sim5$ TeV. The imposed selection

criteria on the C-jets will cause a deviation of such a kind even if the true spectrum is of a single power type. But, as is seen from the simulated results, the deviation caused by the selection criteria is far smaller than that found in the experimental ones. Thus, one may suspect the existence of scanning loss of the C-jets with energy near the minimum value. In order to examine directly the scanning loss and to find out a type of its effect on the analysis, we construct the $\sum E_\gamma - n_\gamma$ correlation diagram shown in Fig. 14. The diagram

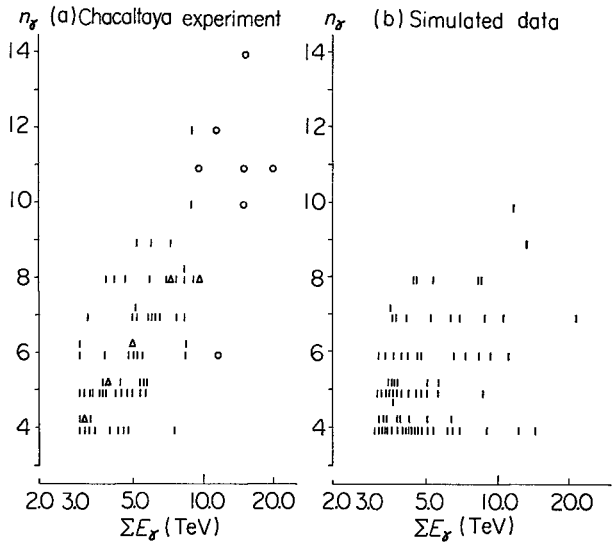

Fig. 14. Correlation diagrams between n_γ and $\sum E_\gamma$.

(a) Chacaltaya experiment, 74 events (normal 62+anormalous (T) 5 denoted with small triangles+two-fire-ball type 7 denoted with small circles).

(b) Simulation experiment with $M_0=2.4$ GeV/c^2. The first half 80 events are plotted here.

of the artificial C-jets is also constructed for comparison, and Fig. 14 presents a half of the artificial C-jets with $M_0=2.4$ GeV/c^2, 80 events, as an example. One now sees that the distribution of the experimental point is less frequent in a region of small $\sum E_\gamma$ and, in particular, of small n_γ value, suggesting the existence of the scanning loss of the events in the region.

To see the effect of this scanning loss on the distribution of $\mathfrak{M}_\gamma$ and of m_γ, we construct a correlation diagram both on $n_\gamma - \mathfrak{M}_\gamma$ and on $n_\gamma - m_\gamma$, shown in Figs. 15 and 16, respectively. From the $n_\gamma - \mathfrak{M}_\gamma$ diagram in Fig. 15, one finds that the distribution of $\mathfrak{M}_\gamma$ does not depend much on a value of n_γ. On the other hand, we have seen from the correlation diagram on $n_\gamma - \sum E_\gamma$ of the artificial C-jets in Fig. 14(b), that the distribution of n_γ does not depend much on a value of $\sum E_\gamma$. Therefore, one may conclude that the $\mathfrak{M}_\gamma$-distribu-

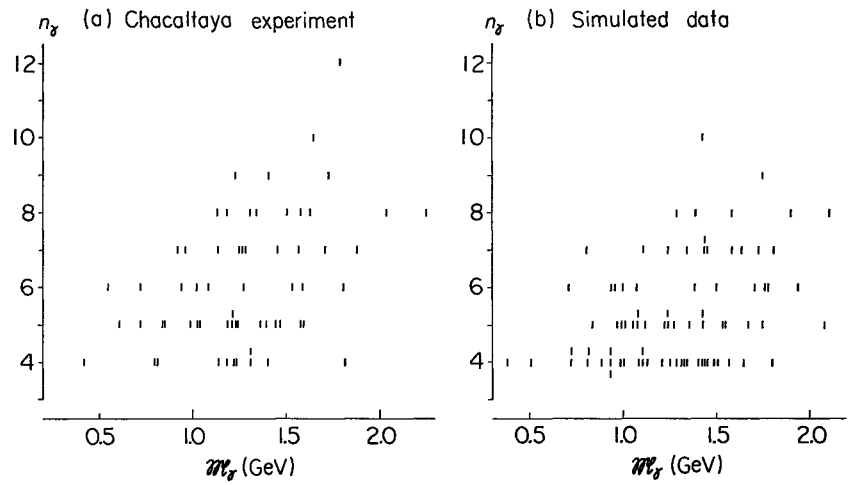

Fig. 15. Correlation diagrams between n_γ and $\mathfrak{M}_\gamma$ (or $\sum E_\gamma^*$).

(a) Chacaltaya experiment. Only 62 normal events are plotted here.

(b) Simulation experiment with $M_0=2.4$ GeV/c^2. The first half 80 events are plotted here.

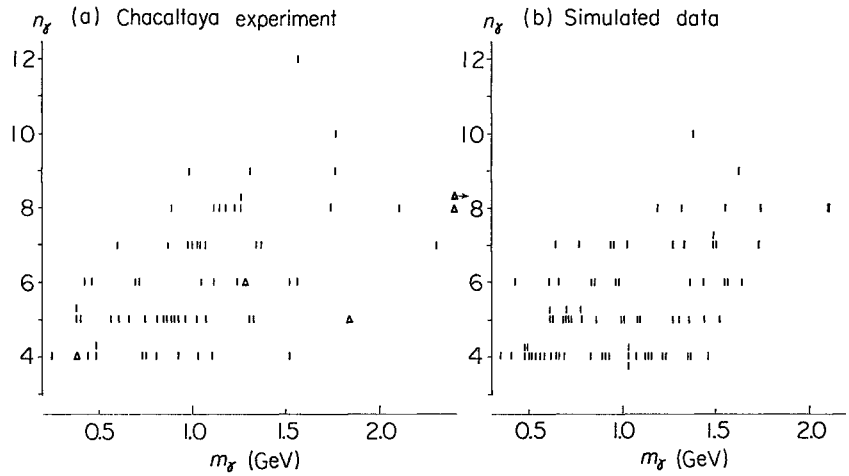

Fig. 16. Correlation diagrams between n_γ and m_γ.

(a) Chacaltaya experiment (normal 62+anormalous (T) 5). Anormalous events are denoted by a small triangle.

(b) Simulation experiment with $M_0=2.4$ GeV/c^2. The first half 80 events are plotted here.

tion will not be seriously affected by the scanning loss of small n_γ and/or small $\sum E_\gamma$ events.

The $n_\gamma - m_\gamma$ correlation diagram, given in Fig. 16, shows a different property. One sees that frequency of events with large m_γ increases as n_γ increases. Therefore, the scanning loss of events with small n_γ will affect the m_γ distribution in such a way that frequency of events with small m_γ will be under-estimated and the average value of m_γ will be over-estimated. But it will make no significant effect on a tail part of the distribution in higher mass region, which is used for the mass estimation.

Thus, one may conclude that the scanning loss will make no serious effect on the mass estimation, which was made with use of $\mathfrak{M}_\gamma$- and m_γ-distribution.

Possible contamination In the design of Chambers 12 and 13 of the Chacaltaya experiment, thickness of the producer layer was determined mainly for obtaining a maximum number of the C-jets. Therefore, the thickness turns out to be too large for accurate and detailed observation on the C-jets. There is not negligible probability of occurrence of successive nuclear interactions in the producer layer, and of occurrence of electromagnetic cascade processes there, too. We cannot deny that effects due to those secondary processes in the producer layer are bringing some troubles in the analysis. For discussions on the successive interactions, we cannot avoid complicated and unsolved problems on the inelasticity. Inversely, the successive interaction is one of the most important objects from which one may be able to draw experimental information on the inelasticity. In the collaboration experiment, the analysis is now under way on the successive interactions with thick chambers and the producer chambers. At this moment, the statistics is not enough to draw a definite conclusion. There are other sources of the contamination, too, for example, mixing of a Pb-jet in the lower chamber among the "γ-rays" of a C-jet. For its accurate estimation, we require better knowledge on the inelasticity, too.

Further, there is some evidence for the existence of the second fire-ball in the multiple production process. A preliminary result of analysis on the second fire-ball is presented in the Appendix of the accompanying paper. But the statistics is not enough and we have to wait for a future analysis for the conclusion. Particles emitted from the second fire-ball have the possibility of being mixed among particles from the first fire-ball, which is the main concern of the present investigation.

We think that it is no point of going further into the detailed quantitative argument at this moment, because processing of a large producer chamber called No. 15 have just been completed and a new analysis is going to be started soon. Therefore, we will confine the present analysis on the artificial C-jets only to such problems, such as to investigate phenomenological

properties of origin of the discrepancy found in the n_γ-distribution, and to present some data which will be useful for a future quantitative analysis on this problem.

From such point of view, we will first discuss the distribution of transverse momentum p_T of γ-rays normalized to one C-jet. A comparison is shown in Fig. 17 between the experimental distribution and the simulated one with $M_0=2.4$ GeV/c^2. In the figure, one sees a difference in a region of small p_T. Therefore, one may think that a part of origin of the discrepancy found in the n_γ-distribution comes from γ-rays of small p_T-value. It makes plausible that the effect of the cascade processes in the producer layer is not eliminated completely in the C-jet data and makes a part of origin of the discrepancy.

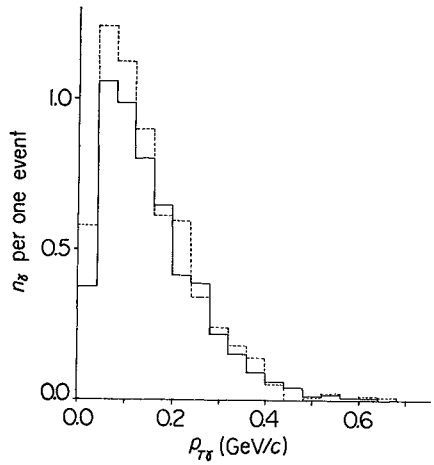

Fig. 17. Comparison of differential $p_{T\gamma}$-distributions in our simulation experiment with $M_0=2.4$ GeV/c^2 (solid line) and in the Chacaltaya experiment (broken line, normal 62+anormalous (T) 5). The number of γ-rays is expressed as per event.

Next, we will go into examination of a decay process of a π^0-meson into two γ-rays. We have a program on the computer to perform the $\pi^0-2\gamma$ coupling procedure on γ-ray data of a C-jet, i.e., to find out a set of pairs of γ-rays out of all possible combination under the condition that the kinematics of $\pi^0-2\gamma$ decay process should give a consistent result to all of pairs in the set.

Applying the coupling procedure to date of the artificial C-jets, two of us (Y. S. and T. Y.) checked the coupling program itself with use of the data on π^0-mesons and we found that the computer gives mis-coupling of the γ-rays seldomly.[4] Now, this coupling procedure by the computer is applied to all data of the observed C-jets and their results are compared with that of the artificial C-jets. Table III gives the number of un-coupled γ-rays per event for both cases. It is interesting to find that the number of the un-coupled γ-rays is slightly larger in the experimental C-jets than that in the artificial C-jets and the difference is nearly equal to the difference found in the average

Table III. Mean number of un-coupled γ-rays per event for C-jets of Chacaltaya experiment and of our simulation experiment.

Chacaltaya experiment	$M_0=2.2$	$M_0=2.4$	$M_0=2.6$	$M_0=2.8$
1.5	0.9	1.1	1.0	1.1

Table IV. Correlation between n_γ and n_{ch} in the artificial C-jets with $M_0=2.4$ GeV/c^2.

Here are shown numbers of events with n_γ γ-rays ($E_\gamma \geqslant 0.2$ TeV) and n_{ch} charged π-mesons ($E_{ch} \geqslant 0.6$ TeV). Figures in the parentheses are those with n_{ch} charged π-meson ($E_{ch} \geqslant 0.6$ TeV).

n_{ch} \ n_γ	2	3	4	5	6	7	8	9	10	Total number of events with n_{ch}
0	—	6 (6)	11 (1)	13 (6)	7(−)	5 (2)	—	1 (−)	—	43(15)
1	—	12 (5)	12 (9)	15 (8)	5 (7)	7 (6)	4 (3)	2 (2)	—	57(40)
2	2 (1)	6 (7)	16(20)	11(12)	6 (8)	7 (6)	3 (3)	1 (1)	—	52(58)
3	2 (2)	2 (4)	4 (9)	5(14)	4 (3)	2 (6)	1 (1)	—	1(−)	21(39)
4	2 (1)	1 (4)	5 (8)	1 (3)	2 (4)	− (1)	1 (2)	− (1)	− (1)	12(25)
5	3 (1)	− (1)	− (1)	1 (3)	3 (4)	—	—	—	—	7(10)
6	− (3)	—	—	2 (1)	− (1)	—	—	—	—	2 (5)
7	—	—	1 (1)	− (1)	1 (1)	—	—	—	—	2 (3)
8	—	—	—	—	—	—	—	—	—	0 (0)
9	− (1)	—	—	—	—	—	—	—	—	0 (1)
Total number of events with n_γ	9	27	49	48	28	21	9	4	1	196
Mean number of charged π-mesons	3.7 (4.9)	1.3 (1.9)	1.7 (2.4)	1.5 (2.4)	2.1 (2.9)	1.3 (1.9)	1.9 (2.2)	1.0 (2.0)	3.0 (4.0)	

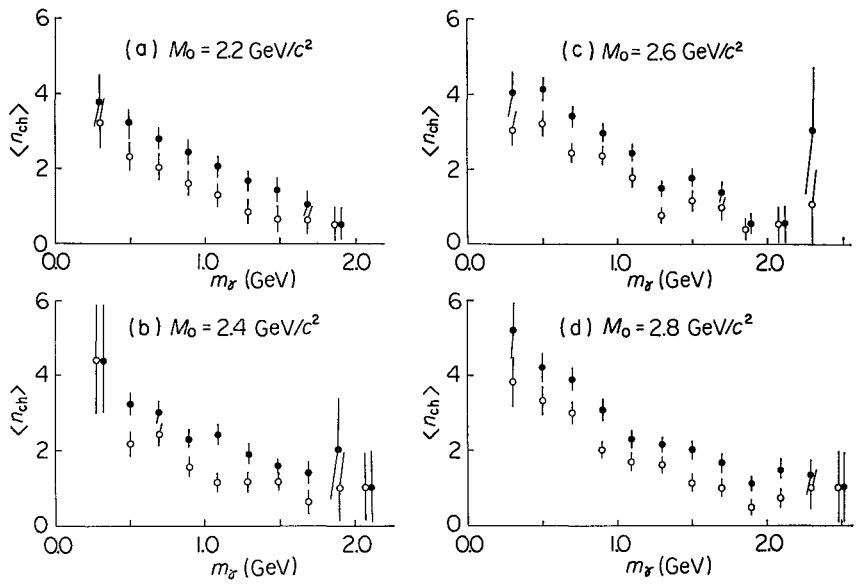

Fig. 18. Correlations between average numbers of charged π-mesons with energies greater than 0.6 TeV (●) or 1 TeV (○) and m_γ.

multiplicity, $\langle n_\gamma \rangle$. From the result, we may think that a part of γ-rays in the C-jet—about 0.4 per event—are contaminations from various sources because they are, in an average, not satisfying the $\pi^0-2\gamma$ kinematics.

Finally, we will look into information on charged π-mesons in the artificial C-jet in order to give estimation of mixing of Pb-jets into "γ-rays" in the C-jets. Table IV presents correlation between number of γ-ray, n_γ, and number of charged particles, n_{ch}. Here the minimum energy is set as $(E_\gamma)_{min}=0.2$ TeV for γ-rays and $E_{ch}=1.0$ TeV and 0.6 TeV for charged π-mesons. In Fig. 18, we present the average number of charged π-mesons, n_{ch}, as a function of the invariant mass m_γ of a C-jet. One sees from them that the number of charged π-mesons n_{ch} is reduced considerably in the C-jets with large invariant mass, m_γ. Therefore, one may conclude that contamination from Pb-jet due to charged π-mesons is, if it exists, not giving serious modification to a tail part of the m_γ-distribution in the higher mass region.

§4. Some problems on C-jet analysis

Moving direction of a fire-ball The emulsion chamber experimet detects only γ-rays among particles produced in the nuclear interaction, and direction of motion of a fire-ball is estimated from data of the observed γ-rays. In the Chacaltaya experiment of the Japan-Brazil collaboration, we computed coordinates of the energy-weighted center of the γ-rays as

$$\begin{aligned} \bar{x} &= \sum E_{\gamma i} x_i / \sum E_{\gamma i}, \\ \bar{y} &= \sum E_{\gamma i} y_i / \sum E_{\gamma i}, \end{aligned} \tag{14}$$

and assumed that location of the energy-weighted center represents direction of motion of the fire-ball. Whereas, in the Bristol-Bombay experiment[5] with the balloon emulsion chamber, they used the squared-energy-weighted center defined below as the center of the event,

$$\begin{aligned} \bar{x} &= \sum E_{\gamma i}^2 x_i / \sum E_{\gamma i}^2, \\ \bar{y} &= \sum E_{\gamma i}^2 y_i / \sum E_{\gamma i}^2. \end{aligned} \tag{15}$$

It is necessary to investigate validity of the assumption, with which direction of motion of a fire-ball is identified to a direction defined by either of the two center above. A study on this problem is made with use of the artificial C-jets. In Fig. 19, we illustrate two examples, one for a case where the assumed center is very close to the real center and the other for the contrary case. A particular attention must be paid to events of such a type where a single γ-ray has much higher energy than all of the rest of γ-rays in an event. In such cases, the emission angle of the highest energy γ-ray can have a large error with any of the proposed methods.

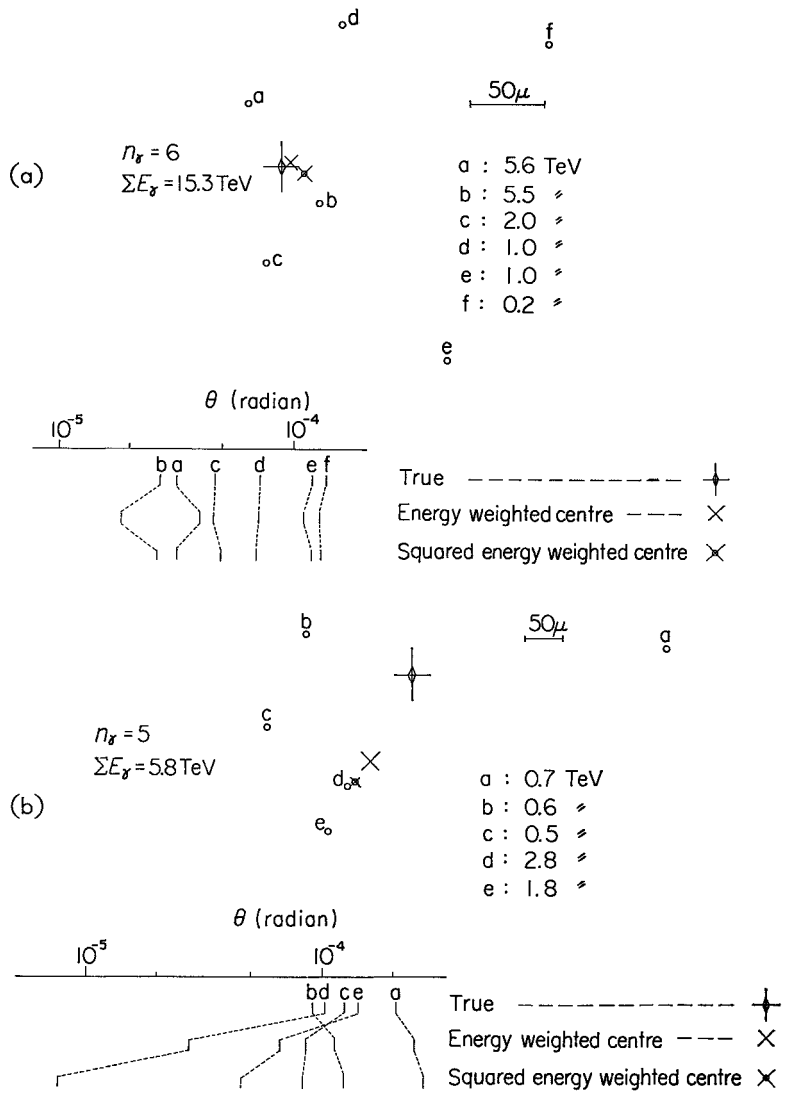

Fig. 19. Typical examples in artificial C-jets, with good (a) or bad (b) correspondence between target diagrm and $\log \tan\theta$-plot. Three $\log \tan\theta$-plot diagrams are made by using the true, the energy-weighted and the squared energy-weighted centers.

In order to present accuracy of determination of direction of motion of a fire-ball in our method of analysis in the Chacaltaya experiment, we construct the angle between the real direction and the approximated direction of motion of a fire-ball in the artificial C-jets. Figure 20 presents distribution of the angle construted in this way.

But, it should be noticed that the present study of the C-jet simulation does not contain any errors caused by the approximated method of the center-

determination, because we applied exactly the same method both for the experimental C-jets and the artificial ones in the comparison.

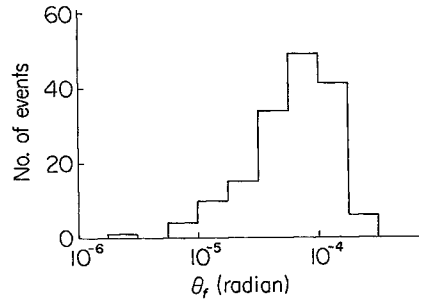

Fig. 20. Distribution of the angle between the true incident direction and the estimated one from the energy-weighted center on the artificial C-jets with $M_0=2.4$ GeV/c^2.

Torpedo Reanalysis of the data of balloon emulsion chamber experiment of the Bristol-Bombay collaboration[5] was made in the same way as in the Chacaltaya experiment. The result shows in the Bristol-Bombay data existence of two types of C-jets other than those which show emission of a fire-ball with mass $2\sim3$ GeV/c^2 —emission of a H-quantum. One of the two is the events which are interpreted as emission of a fire-ball of very large mass, $20\sim30$ GeV/c^2—emission of a SH-quantum. The other is the one named "torpedo" which are characterized by the existence of one or two γ-rays emitted in very forward direction with small angles and with energy much greater than the rest of produced particles. The former type of events—SH-quantum type—was discovered first and was mainly investigated by the A-jet analysis of the Chacaltaya experiment. In the C-jet analysis of the Chacaltaya experiment, we recognized the existence of both types of the events, but their frequency was found rather small as shown in Table I, one event of the SH-quantum type and 5 events of the torpedo-type.

As is clear by its definition, the "torpedo" event has the correlation diagram of $\sum_\theta E_\gamma-\theta_\gamma$ and $\sum_\theta p_{T\gamma}-\theta_\gamma$ with a completely different shape from that of the isotropic emission. What is more interesting is, if one takes one or two characteristic γ-rays of very high energy out of the event, then the rest of γ-rays are always in good agreement with the expected distribution of the isotropic emission. As is shown in the above consideration on determination of the center of a fire-ball, estimation on emisson angle of the very energetic γ-rays can be with a serious error due to uncertainty of location of the center. Therefore, characteristics of the torpedo-type event seen in the energy spectrum will be more reliable basis than the angular distribution for investigation on the torpedo.

One is able to make an estimation on frequency of an event where a single γ-ray happens to have much larger energy than the rest, simply due to the fluctuation. Let us express energy of γ-rays of the highest and the second highest as E_1 and E_2, respectively. We construct distribution of the ratio E_2/E_1 and present the result in Fig. 21, for the artificial C-jets, for C-jets of the Chacaltaya experiment, and for the C-jets of the Bristol-Bombay experiment.

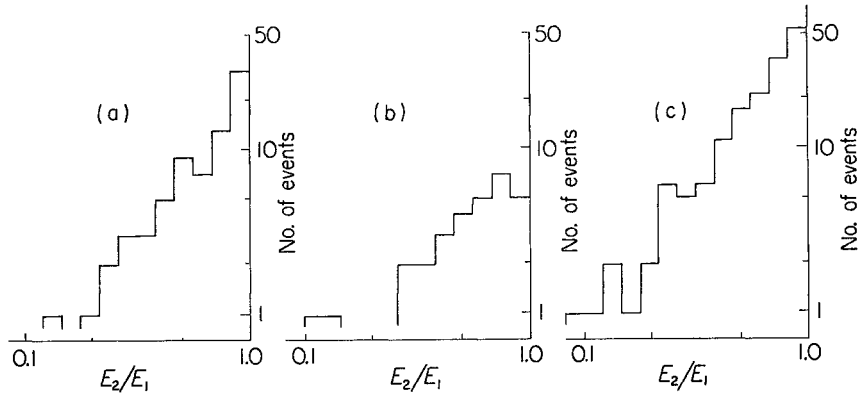

Fig. 21. Distribution of the ratio E_2/E_1, where E_1, E_2 are the highest and the second highest energies of γ-rays in a C-jets.
(a) Chacaltaya experiment. (b) Bristol-Bombay experiment.
(c) Our simulation experiment with $M_0=2.4$ GeV/c^2.

In applying the analysis to the Bristol-Bombay data, we imposed the selection criteria as $E_\gamma \geq E_{\min}=0.1$ TeV, $\sum E_\gamma \geq 1.5$ TeV and $n_\gamma \geq 4$, which was made to maintain a similarity relation with the analysis of the Chacaltaya experiment, i.e. $(\sum E_\gamma)_{\min}/E_{\min}=15$ for both cases. After application of the criteria, number of the torpedo events in the Bristol-Bombay experiment is reduced to two, and the two are characterized by the inequality as, $E_2/E_1 \leq 0.3$.

Now in Fig. 21, one sees no significant difference in the E_2/E_1 distribution for the three cases. Therefore, we have to wait future experiment for conclusion on the torpedo problem, because the present experimental evidences are yet not much beyond the expected fluctuation. Further, one may point out that the emulsion chamber in the Bristol-Bombay experiment has not enough space between the graphite producer layer and the emulsion chamber itself to separate cascade showers caused by individual γ-rays emitted in very forward angular region. This may be a cause of a slight difference found in the distribution in the region near $E_2/E_1 \sim 1.0$.

Check for individual C-jets So far, we discussed the two quantities, $\mathfrak{M}_\gamma$ and m_γ, particularly about shape of their respective distribution without paying attention to their mutual correlation. It was already pointed out that estimation of $\mathfrak{M}_\gamma$ may not be completely free from a subjective error, though the quantity $\mathfrak{M}_\gamma$ should be in principle identified to the energy sum in the fire-ball rest system, $\sum E_\gamma^*$, after extrapolation of the data below the detection threshold. In order to see the situation clearly, we construct a correlation diagram on $\mathfrak{M}_\gamma - m_\gamma$ for the C-jets of the Chacaltaya experiment and on $\sum E_\gamma^* - m_\gamma$ for the artificial C-jets of the simulation experiment. In the experimental $\mathfrak{M}_\gamma - m_\gamma$ diagram, we omitted few anormalous events out of the statistics because we require both values of $\mathfrak{M}_\gamma$ and m_γ for the diagram. Those

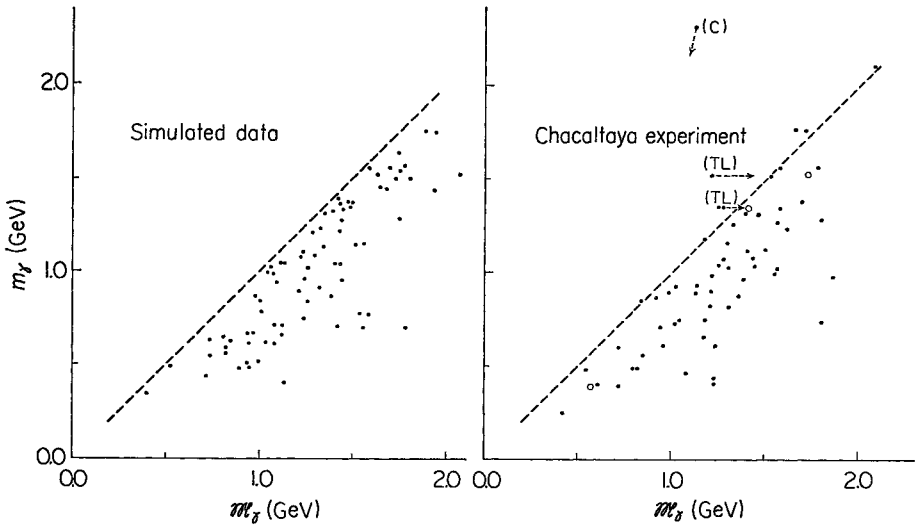

Fig. 22. Correlation diagram between $\mathfrak{M}_\gamma$ (ΣE_i^*) and m_γ.

(a) Chacaltaya experiment. Only 62 normal events are plotted. The symbols (C) and (TL) denote events with special features and mean an event with contamination and torpedo-like events, respectively. In this figure, circles mean corrected positions.

(b) Our simulation experiment with $M_0=2.4$ GeV/c^2. Here are plotted the first half 80 events.

are either of the torpedo type (no estimation is given on $\mathfrak{M}_\gamma$) or of the two-fire-ball type (no value is given for m_γ). As is seen from the result shown in Fig. 22, the points of the simulated C-jets are distributed below a straight line of 45° as is evident from the definition. The distribution of points of the experimental C-jets, on the other hand, shows that the large part is below the 45° line, the allowed region, while a few events above, in the forbidden region. It is important to look in more detail of the C-jet events which lie far above the 45° line, in the forbidden region.

The farthest point in the diagram (denoted by C) represents the event, Waseda 24-11. A map of the event is shown in Fig. 23, from which one recognizes existence of one particular γ-ray f(0.4 TeV), lying at a distance as large as 1.84 mm from the center of the rest of six γ-rays. Because of this particular feature, value of the invariant mass m_γ turns out to be very large. While in estimation of

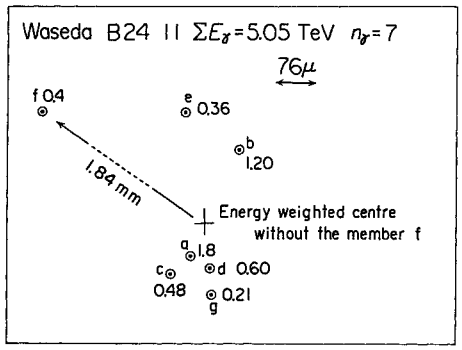

Fig. 23. Map of an event interpreted as that with contamination, which is denoted by symbol (C) in Fig. 22. This event was re-analyzed by omitting γ-ray of member f.

$\mathfrak{M}_\gamma$, the curve fitting is made with more attention to the central six γ-rays than the particular γ-ray f so as to maintain consistency with the isotropic emission hypothesis. This naturally yields small estimated value for $\mathfrak{M}_\gamma$. We know nothing on origin of this particular γ-ray f, but it may well be a contamination from some sources. If one takes out the γ-ray f and reanalyze the event once again, we obtain the result shown by a circle in the diagram.

Among the rest of events in the forbidden region, the two (assigned with TL in the diagram), INS 23-62 and Waseda 25-7, are like the torpedo type. Figure 24 presents the $\sum_\theta E_\gamma - \theta_\gamma$ and $\sum_\theta p_{T\gamma} - \theta_\gamma$ correlation diagram of those two events. The broken curve in the figure represents the so-called best-fitted ones which are determined in the analysis of the Chacaltaya experiment. Now, we can pick up some examples of the artificial C-jets which exhibit the torpedo-like feature. Two of such examples are illustrated in Fig. 25, where we plot together the corresponding curves with correct values of $\sum E_\gamma^*$ and the γ-factor for a comparison. It is seen that the correct curves are not always the so-called best-fitted ones, particularly in the torpedo-like events. If one re-adjust the curve-fitting in the two events following the situation exhibited by the artificial torpedo-like events, one will obtain a curve like that shown by a solid line. This re-fitting of the curve gives revised estimation of $\mathfrak{M}_\gamma$ for the two C-jets, both of which lie in the allowed region.

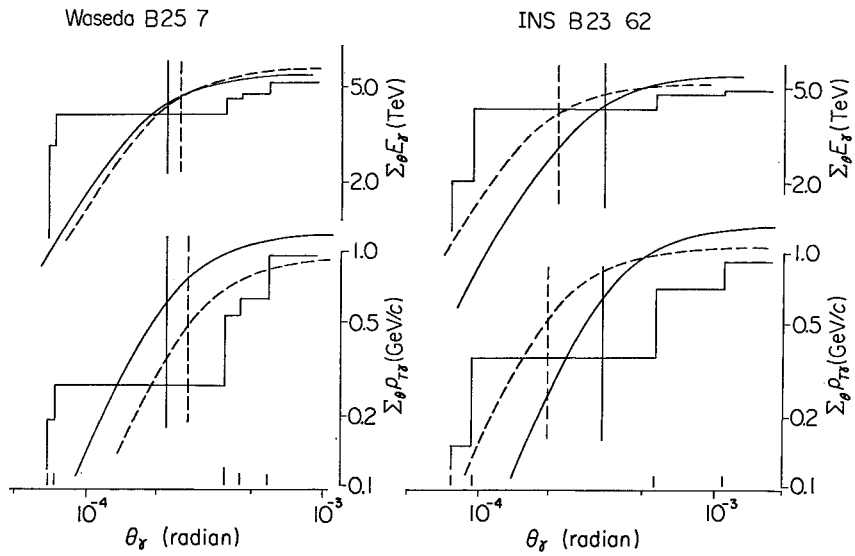

Fig. 24. Correlation diagrams of $\sum_\theta E_T - \theta_T$ and $\sum_\theta p_{T_T} - \theta_T$ of torpedo-like events. Broken curves are theoretical curves fitted in the earlier analysis and solid curves are those re-fitted by the aid of the text shown in Fig. 25.

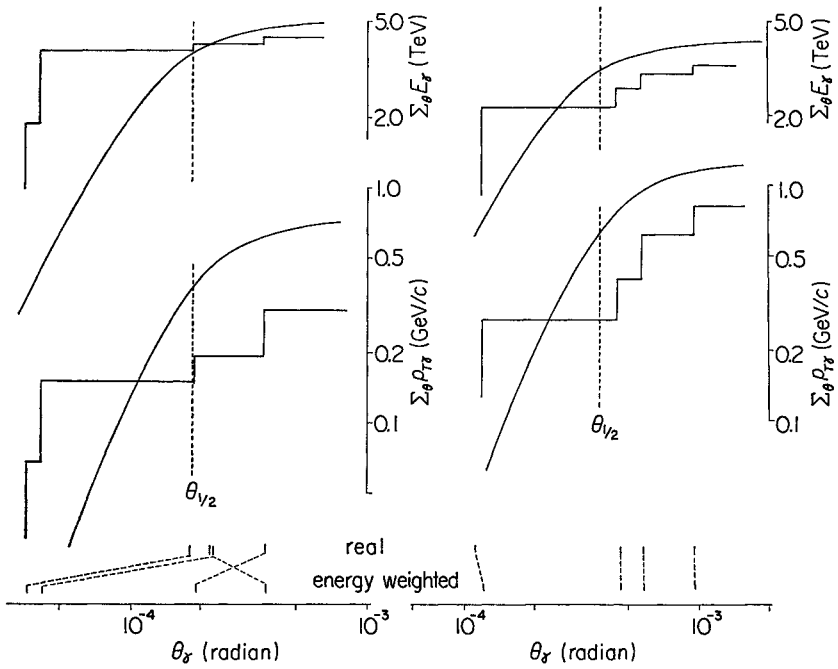

Fig. 25. Examples of $\sum_\theta E_\gamma$-θ_γ and $\sum_\theta p_{T\gamma}$-θ_γ diagrams of torpedo-like artificial C-jets. Theoretical curves are fitted correctly. Log tan θ_γ-plot diagrams are also shown in the lower part with use of the true incident direction and that estimated from the energy-weighted center.

Now, we can compare the revised correlation diagram of $\mathfrak{M}_\gamma - m_\gamma$ with the diagram of $\sum E_\gamma^* - m_\gamma$ of the artificial C-jets. For the comparison, we construct a histogram on $(\mathfrak{M}_\gamma - m_\gamma)/\mathfrak{M}_\gamma$ from the experiment and on $(\sum E_\gamma^* - m_\gamma)/\sum E_\gamma^*$ from the simulation. Figure 26 shows both of the histograms, the former one by a broken line and the latter by a solid line. As a whole, we have an impression of over-estimation of several % in experimental evaluation on $\mathfrak{M}_\gamma$, though we have already seen that $\mathfrak{M}_\gamma$ can be under-estimated several ten % sometimes in a torpedo-like event. But we think that the quantitative conclusion is better to be postponed, because the $\mathfrak{M}_\gamma$ estimation could have a large error in some type of a C-jet as we have learned from the simulation examples.

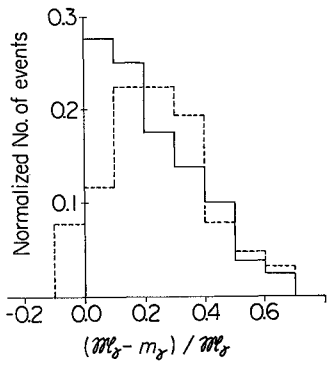

Fig. 26. Distribution of the relative deviations $\mathfrak{M}_\gamma - m_\gamma/\mathfrak{M}_\gamma$. Broken and solid lines correspond to the Chacaltaya experiment and our simulation experiment with $M_0 = 2.4$, respectively.

§5. Conclusion and summary

We performed a simulation experiment by a computer on the observation of C-jets with a producer chamber. In the simulation of a fire-ball, we made several simple assumptions on its physical properties on the basis of the experimental knowledge so far obtained. Data of the artificial C-jets are reproducing very well results of the statistical analysis in the Chacaltaya experiment, such as $\sum E_\gamma$-spectrum, $p_{T\gamma}$-distribution, $E_\gamma/\sum E_\gamma$-distribution and so on.

A significant result of the simulation experiment is a large fluctuation of physical quantities of the artificial C-jets. The ratio $\sum E_{ch}/\sum E_\gamma$ has large fluctuation, too, which comes originally from the charge fluctuation of π-mesons emitted from a fire-ball, with complicated amplification due to the imposed selection criteria ($E_{min}=0.2$ TeV and $\sum E_\gamma \geq 3$ TeV and $n_\gamma \geq 4$). Therefore, estimation of mass-value of a fire-ball in the individual events cannot be obtained simply by multiplying a constant factor to its γ-ray mass, i.e., a part of the rest-energy given to γ-rays. The best estimation of the mass-value can be obtained through comparison of the experimental results with the corresponding simulation results on various physical quantities. Here the simulation experiment with the artificial C-jets must be made under the exactly identical conditions with those in the actual experiment.

Results of the comparison are as follows. Expressing mass of a fire-ball as M_0, we obtained $M_0=2.4$ GeV/c^2 from distribution of the γ-ray mass, $\mathfrak{M}_\gamma$, and $M_0=2.2\sim2.6$ GeV/c^2 from distribution of the invariant mass of γ-rays, m_γ. Comparison on distribution of the γ-ray multiplicity n_γ, prefers a value $M_0=2.8$ GeV/c^2. The last quantity, n_γ, which is less directly connected to the fire-ball mass than the first two, $\mathfrak{M}_\gamma$ and m_γ, gives us a slightly different estimation on M_0.

Now discussion gives into examination on possible sources of systematic errors in the experiment, which may bring distortion of the experimental data and cause such discrepancy as the above. Here one can think of the following two major sources.

One is the scanning loss of the events near the border lines of the selection criteria, existence of which can be inferred from a bend of the oberved $\sum E_\gamma$-spectum near the minimum value. The other is mixing of the contamination from various sources into γ-rays of the C-jets. One may suspect existence of the contamination simply from slightly larger experimental value of the γ-ray multiplicity than that expected from $\mathfrak{M}_\gamma$ and m_γ.

The former source of errors is rather simple in its character, and we are able to estimate its effect on various distributions. Whereas, the situation on the latter source of errors is quite complicated and large thickness of the producer layer of Chambers 12 and 13 enhanced effects of this type of sources in various respects. Thus, the best will be to wait the experiment with a

new chamber No. 15, which has a large area and thin producer layer. Here, we will be satisfied only with its phenomenological investigation.

Both of the two types of sources of a systematic error give direct effect on distribution of the γ-ray multiplicity n_γ, but not so much on distribution of the invariant mass, m_γ. In particular, a tail of the m_γ-distribution in larger mass region is least affected by the sources, and we use the tail part for the mass estimation. A conclusion on the mass estimation is derived from comparison of the distribution on $\mathfrak{M}_\gamma$, m_γ and n_γ and an argument on the sources of systematic errors. The result is that M_0 lies in an interval of 2.2~2.6 GeV/c^2. This is the present best value for the rest mass of the H-quantum.[3]

There are some more problems in an analysis of cosmic-ray experiments of the emulsion chamber type. One is a method of determination of the center of an event and of direction of motion of a fire-ball. This point brings no problem to the present mass estimation, because we applied the same method of the center determination both for the experimental and artificial C-jets. But, effects from the method cannot be overlooked, when we are discussing on existence of some particular types of the event, for example the torpedo-type event with emission of one or two γ-rays carrying most part of the total energy into a very forward direction.

For existence of a large fire-ball, re-analysis of the data of the Bristol-Bombay experiment showed a number of examples with emission of a fire-ball of mass 20~30 GeV/c^2—SH-quantum—in the energy region concerned here. Effect of mixing of this type of events on the present mass estimation can be regarded as a part of the contamination discussed above. In the Chacaltaya experiment, we identified one SH-quantum event among the observed C-jets, as shown in Table I of the accompanying paper.

Finally, we would like to point out a characteristic of the present simulation experiment. We asked the simulated examples to satisfy rigorously the conservation law of energy and momenta, and required rest energy of a simulated fire-ball to lie in a narrow interval around the assigned mass value, $M_0 \pm 0.05$ GeV/c^2. These strict conditions were imposed in order to avoid unnecessary complications and ambiguous factors coming into the results besides the basic assumption, though they require far larger amount of effort and computer time. In fact, through this effort, we are able to find such fact that the experimental $\mathfrak{M}_\gamma$-distribution has a maximum with width as small as the simulated one computed with the narrow mass distribution.

Acknowledgement

The authors would like to express their sincere thanks to Prof. Y. Fujimoto for his kind help in writing the manuscript and for his enlightening discussion and comment.

The simulation calculation was made with use of a computer, FACOM 270–30, of the Institute of Physical and Chemical Research.

References

1) Japanese and Brazilian Emulsion Chamber Groups, Prog. Theor. Phys. Suppl. No. 47 (1971), 1.
2) S. Hasegawa, H. Nanjo, T. Ogata, M. Sakata, K. Tanaka and N. Yajima, Prog. Theor. Phys. Suppl. No. 47 (1971), 126.
3) S. Hasegawa, Prog. Theor. Phys. **26** (1961), 150; **29** (1963), 128.
4) Y. Sato and T. Yanagita, Uchusenkenkyu (mimeographed circular in Japanese) **14** (1970), 390.
5) P. K. Malhotra, P. G. Shulka, S. A. Stephens, B. Vijayalakshmi, J. Boult, M. G. Bowler, P. H. Fowler, H. L. Hackforth, J. Keereetaveep, V. M. Mayes and S. N. Tovey, Nuovo Cim. **40A** (1965), 404.